In situ IR pyrometric analysis during thermal treatment in air of TiO_xN_y coatings

F.-D. Duminica, F. Maury *

CIRIMAT, CNRS/INPT/UPS, ENSIACET, 118 Route de Narbonne, 31077 Toulouse cedex 4, France

Abstract

IR pyrometry is an original diagnostic tool for in situ analysis of surface transformations of coatings or bulk materials during the thermal treatment under reactive atmosphere such as high temperature oxidation. Significant oscillations of the pyrometric signal were observed during annealing in air of $TiO_{1.5}N_{0.5}$ coatings in the temperature range 673–823 K. This is due to interferences resulting from multi-reflections at the interfaces of a transparent growing film. This reveals the formation of a TiO_2 thin film on the top of the $TiO_{1.5}N_{0.5}$ coating. Modeling of the time dependence of the IR pyrometric signal allows the determination of the oxide layer thickness, transformation rate and optical properties of the films under the growth conditions. The progressive oxidation of a compact amorphous $TiO_{1.5}N_{0.5}$ coating from the external surface to the substrate interface was supported by SIMS, XRD and reflectance analyses.

Keywords: IR pyrometry; TiO_xN_y coatings; High temperature oxidation; In situ analysis; Surface diagnostic

1. Introduction

In addition to its first functionality which is the temperature measurement of a body, IR pyrometry can be used as an original surface diagnostic tool for CVD and related processes to detect and to analyze the dynamics of any events occurring on the surface during the growth. The great sensitivity of this technique makes possible the detection of surface phenomena and in situ control of growth processes with the advantage of a particularly simple and low cost technique, working in the specific ambient of CVD processes, even under atmospheric pressure since low pressures are not necessary for this optical analysis. Since the pioneering works of Pigeat et al. on the emissivity of tungsten during oxidation at high temperature [1] IR pyrometry was used for instance to study the germination of diamond [2,3] and to determine the growth rate in a microwaves plasma process [3–6]. It was also used during MBE growth of partially opaque layers of III–V semiconductors [7,8]. In previous papers, we have shown that IR pyrometry offers great potentialities since it could be applied in various CVD processes for real time monitoring of the growth of a wide variety of thin film materials [9–12]. Indeed, in situ IR pyrometry was used during the CVD of Cr-based barrier layers [9,10], to study the growth mechanisms of Fe by MOCVD [11] and, recently, to monitor the deposition of transparent oxide layers [12]. Fundamentals and modeling of the emissivity of layer-substrate couples were reported [5,13]. The development of pyrometric models is still in progress for instance to analyze in situ the optical properties of thin films during the growth process, as reported by a recent work published in the course of the present paper [14].

In this paper, the technique is not used to control a CVD process but to analyze in situ the oxidation at high temperature of amorphous $TiO_{1.5}N_{0.5}$ coatings which are candidates for protective metallurgical applications. It is shown that IR pyrometry provides fruitful informations on the formation of anatase (and rutile) TiO_2 during thermal treatments under air of these coatings in the temperature range 673–823 K.

2. Experimental

The $TiO_{1.5}N_{0.5}$ coatings were deposited in a cold-wall vertical CVD quartz reactor, 5 cm in diameter, using a process described elsewhere [15]. The same reactor was used for the thermal treatment under air of these coatings. The samples were placed on a stainless steel sample holder (3.2 cm in diameter)

* Corresponding author. Tel.: +33 562885669; fax: +33 562885600.
E-mail address: francis.maury@ensiacet.fr (F. Maury).

doi:10.1016/j.surfcoat.2007.07.051

heated by HF induction. The annealing temperature was measured using a thermocouple inserted in the sample holder. A monochromatic IR pyrometer ($\lambda = 1.6$ μm; AOIP TR7020E model) was used to monitor the radiation emitted by the sample through the quartz wall of the reactor at an incidence of approximately 30° compared to the normal. The $TiO_{1.5}$ $N_{0.5}$ coatings were deposited on stainless steel and for some specific characterizations on Si(100). Their typical thickness was fixed around 1 μm. Unless otherwise specified, the emissivity coefficient of the IR pyrometer was maintained at the value of stainless steel ($\varepsilon = 0.21$). The intensity of the pyrometric signal versus time was collected with a computer. If the total emissivity of the film/substrate system was known, the real temperature could be determined from the pyrometric signal. The spectral emissivity depends on the material and, generally, metals exhibit lower values than oxides. As a result, the pyrometric signal is sensitive to changes of emissivity during the thermal treatment and the measured value corresponds to an apparent temperature as previously discussed [9].

3. Results and discussion

3.1. Film characterization and in situ IR pyrometric diagnostic

The growth of $TiO_{1.5}N_{0.5}$ coatings was performed by atmospheric pressure CVD at 673 K as previously reported [15]. As-deposited films exhibit a high compactness, a smooth surface morphology and an amorphous XRD structure. Fig. 1 shows SEM micrographs of a 1 μm thick $TiO_{1.5}N_{0.5}$ coating grown on stainless steel. The film is dense and uniform and it exhibits a metallic aspect. The surface roughness (rms) of the film determined by optical profilometry was approximately 20 nm. These coatings are candidates for corrosion protection and also as barrier underlayers prior to the deposition of functional thin films on steel in order to prevent the diffusion of elements from the substrate. Indeed, it is known for instance that TiN is a better interdiffusion barrier when it contains significant amounts of oxygen [16].

In order to study the thermal stability of these coatings, they were annealed under air in the temperature range 623–823 K for different times. For temperatures lower than 673 K the

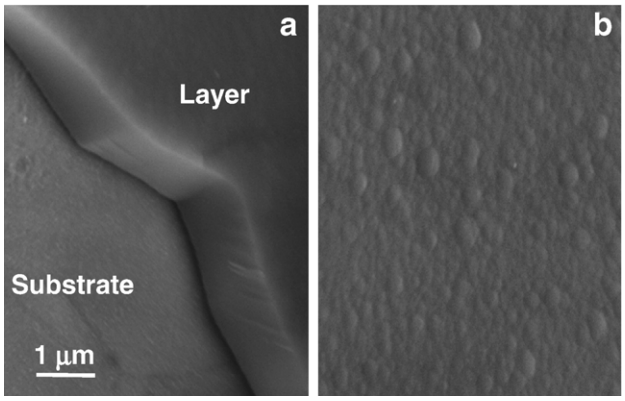

Fig. 1. SEM micrographs of a $TiO_{1.5}N_{0.5}$ coating grown on stainless steel: a) tilted image showing the cross-section; b) surface morphology.

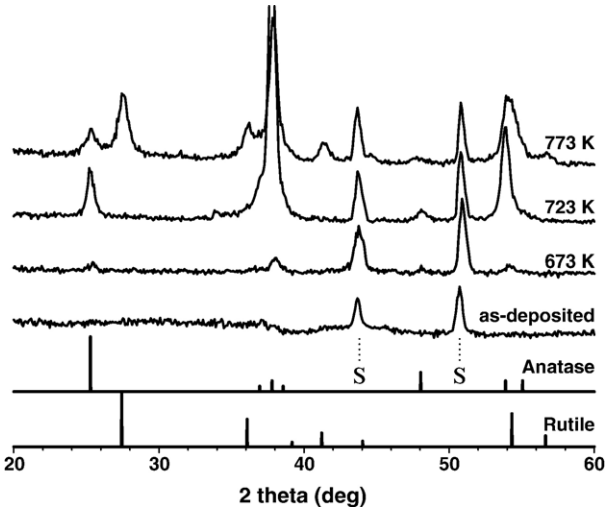

Fig. 2. XRD grazing patterns (incidence angle 2°) of an amorphous as-deposited $TiO_{1.5}N_{0.5}$ film and of coatings after annealing in air in the temperature range 673–773 K for 210 min (The peaks from the substrates are marked S).

$TiO_{1.5}N_{0.5}$ films exhibit a relatively good thermal stability under air during four hours since no change was observed in the XRD patterns (data not shown). Fig. 2 shows the effect of the thermal treatment in the range 673–823 K under air for 240 min of 1 μm thick amorphous $TiO_{1.5}N_{0.5}$ coatings. At 673 K an oxidation starts slowly and traces of crystalline TiO_2 anatase is observed after 210 min. By increasing the temperature at 773 K the oxidation rate increases and rutile crystallizes to the detriment of anatase.

During the annealing of as-deposited $TiO_{1.5}N_{0.5}$ film, the temporal variation of the IR pyrometric signal shows different profiles depending on the annealing temperature (Fig. 3). At 673 K the signal is almost constant during four hours, while for temperatures equal and higher than 723 K oscillations are observed with a period that depends on the annealing temperature. At 723 K the oscillations appear over 150 min and are followed by a stabilization of the pyrometric signal to a constant

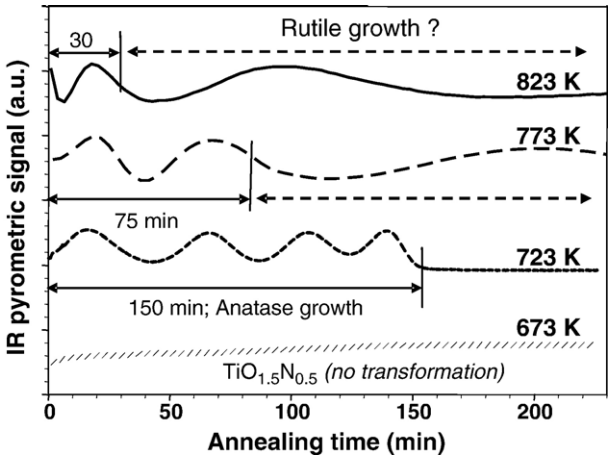

Fig. 3. In situ variation of the IR pyrometric signal with the annealing time at different temperatures during annealing in air. The time range corresponding to the growth of anatase is marked with an arrow and the one corresponding probably to rutile with a dotted arrow.

value which remains unchanged for more than 5 h. Increasing the temperature at 773 K the behavior of the pyrometric signal is slightly different since oscillations are observed over a shorter time (75 min) and they are followed by other oscillations with lower amplitude and a drastically longer period. A similar behavior is observed at 823 K with again two regimes, clear oscillations in the early stages (30 min) with a short period followed by oscillations with a significantly longer period and lower amplitude.

In order to understand the origin of these different oscillations we particularly focus on the thermal treatment at 723 K. From Fig. 2 we know that TiO_2 anatase is formed after 210 min. SIMS depth profiles of $TiO_{1.5}N_{0.5}$ coatings annealed for different times reveals clearly that nitrogen is removed from the surface of the film to form a TiO_2 top layer (Fig. 4). Interestingly the interface between TiO_2 and $TiO_{1.5}N_{0.5}$ is sharp and it moves progressively toward the substrate as the oxidation time increases. After 210 min the nitrogen is completely evolved excepted traces at the interface with the substrate probably due to its roughness (rms=40 nm) or to a possible N diffusion in the steel during the deposition.

3.2. Modeling of the pyrometric signal

At this stage, it is established that $TiO_{1.5}N_{0.5}$ coatings oxidize to form TiO_2. As a result, the pyrometric signals of Fig. 3 contain informations on this transformation, especially the trace recorded at 723 K where only anatase is formed (Fig. 2) and a single set of oscillations is observed. We suppose the transformation of $TiO_{1.5}N_{0.5}$ into TiO_2 occurs by a linear displacement of the oxidation interface with the annealing time at 723 K in agreement with literature results [17]. Then, using a model developed previously for the growth of TiO_2 on different substrates [12] and directly derived from the Yin's model [5], we have simulated the pyrometric signal for the growth of TiO_2 on $TiO_{1.5}N_{0.5}$ film. Fig. 5 shows a comparison between experimental and theoretical variations of the pyrometric signal. The adapted model fits quite well with the experimental trace. The

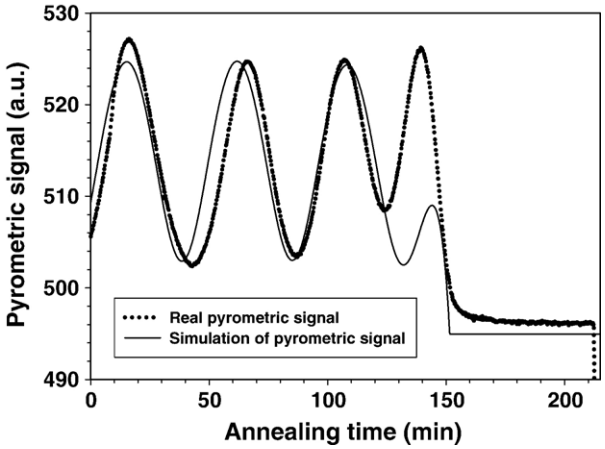

Fig. 5. Temporal variation of the experimental pyrometric signal (dotted line) and simulated pyrometric signal (full line) during the annealing of a $TiO_{1.5}N_{0.5}$ (1000 nm) coating at 723 K under air. Data resulting from calculation: $n_{TiO2}=2.5$; $n_{TiO1.5N0.5}=3$; $k_{TiO2}=9\cdot10^{-4}$; $k_{TiO1.5N0.5}=4\cdot10^{-1}$; TiO_2 growth rate=6.6 nm/min. The surface roughness does not change after the thermal treatment (rms=20 nm).

data resulting from the simulation are: refractive index $n_{TiO2}=2.5$ and $n_{TiO1.5N0.5}=3$; extinction coefficient $k_{TiO2}=9\cdot10^{-4}$ and $k_{TiO1.5N0.5}=4\cdot10^{-1}$; TiO_2 growth rate=6.6 nm min^{-1}. The surface roughness was maintained constant for the fitting to the value measured after the annealing treatment (rms=20 nm). The optical parameters of $TiO_{1.5}N_{0.5}$ recently reported [17] and the emissivity of both TiO_2 and $TiO_{1.5}N_{0.5}$ films previously determined were used as input data. The optical parameters of $TiO_{1.5}N_{0.5}$ used in the model are in good agreement with those reported for similar films grown using other deposition processes [17,18].

During the annealing, the emissivity of the pyrometer was fixed at 0.21 (typical value of the stainless steel). The high difference between the substrate and film emissivity ($\varepsilon TiO_{1.5}N_{0.5}=0.65$) explains the significant variation of the pyrometric signal in the first minutes of the heating treatment compared to the real sample temperature fixed at 723 K. The

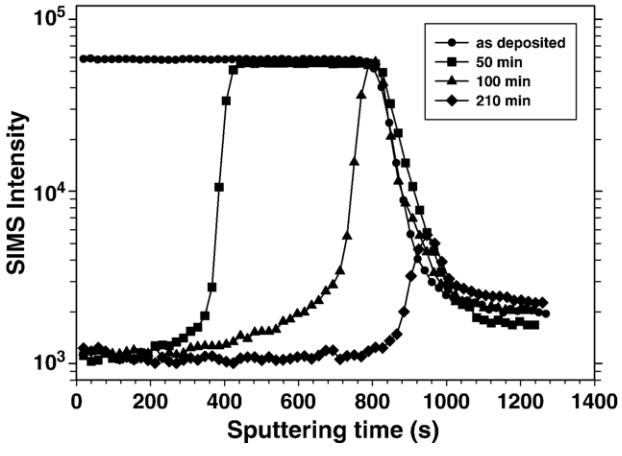

Fig. 4. SIMS concentration depth profiles of nitrogen for as-deposited and different $TiO_{1.5}N_{0.5}$ films annealed in air at 723 K for different times (50, 100 and 210 min).

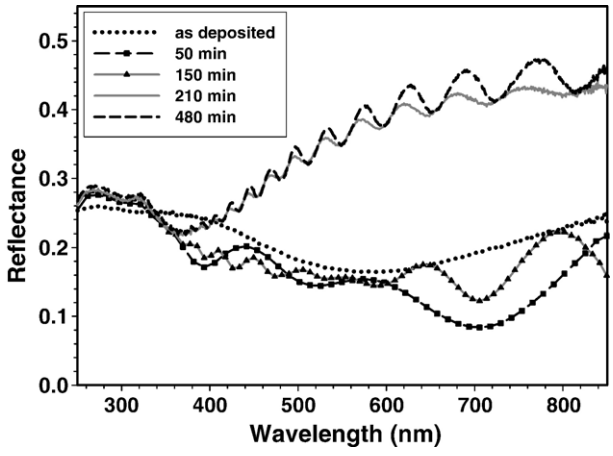

Fig. 6. Reflectance spectra of $TiO_{1.5}N_{0.5}$ films grown on stainless steel substrate after different annealing times under air at 723 K. The oscillation period of films annealed after 210 and 480 min is equivalent, indicating that both films have the same TiO_2 thickness.

abrupt change of the pyrometric signal after 150 min is due to the complete transformation of $TiO_{1.5}N_{0.5}$ into TiO_2 anatase. The constant value of the IR pyrometric signal after 150 min confirms that no further structural and chemical change occurs: anatase is stable under these conditions. Near the end of the oxidation, the discrepancy observed between experimental and simulated curves (last oscillation) could be due to various parameters that were not considered in the model, as for instance the roughness of the $TiO_2/TiO_{1.5}N_{0.5}$ interface resulting from interdiffusion or to local changes in the nitrogen content which would affect the optical properties. After oxidation, the microstructure of the coating does not change significantly. The resulting TiO_2 film is compact with a smooth surface morphology and it exhibits optical properties very close to those of bulk anatase ($n=2.5$, $k=10^{-3}$ for wavelength $\lambda=600$ nm). Modeling of reflectance spectra of TiO_2 films discussed in the next section will confirm these results.

3.3. Comparison with ex situ reflectance data

During annealing in air at 723 K the color of the $TiO_{1.5}$ $N_{0.5}$ film changed gradually from metallic dark grey to yellowish after 150 min. This observation was correlated with reflectance spectra recorded at different annealing times (Fig. 6). As-deposited $TiO_{1.5}N_{0.5}$ coating is opaque and the reflectance is about 20% in the wavelength range 400–800 nm; no oscillations are observed. This is in agreement with the relative high extinction coefficient ($k=4\cdot10^{-1}$) characteristic of mid-gap semiconductors ($E_g=2$ eV) [17]. Upon oxidation, a transparent anatase TiO_2 layer with low extinction coefficient ($k=9\ 10^{-4}$) is formed, multi-reflections at the interfaces occur and interference fringes readily appear with a period decreasing by increasing the annealing time and thus the TiO_2 thickness. The reflectance spectra of the samples oxidized for less than 200 min exhibit the features of duplex $TiO_{1.5}$ $N_{0.5}/TiO_2$ coatings while for longer oxidation times the films are completely oxidized and the reflectance increases above 40% in the wavelength range 600–800 nm. These coatings exhibit the same period and subsequently the same TiO_2 thickness giving evidence for a complete oxidation. The TiO_2 thicknesses determined by modeling the reflectance spectra using a procedure previously described [19] reveals a linear increase with the annealing time (Fig. 7). The oxidation rate is approximately 6 nm min^{-1} in good agreement with the values obtained using the equation proposed by Spring Thorpe [8] which is included in the above simulation model of the pyrometric signal.

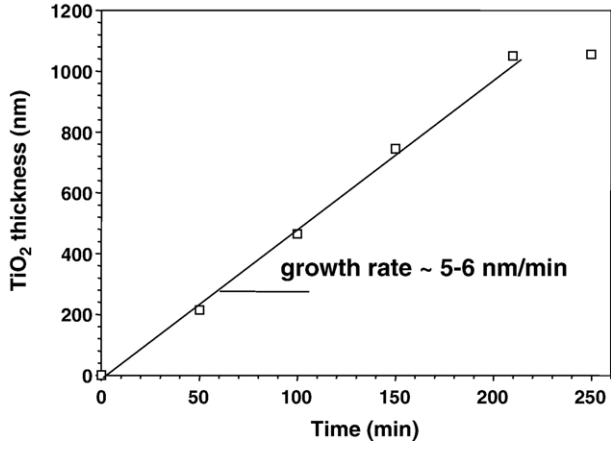

Fig. 7. Variation of TiO_2 thickness with the annealing time at 723 K under air of $TiO_{1.5}N_{0.5}$ coatings. Thicknesses were determined from reflectance spectra.

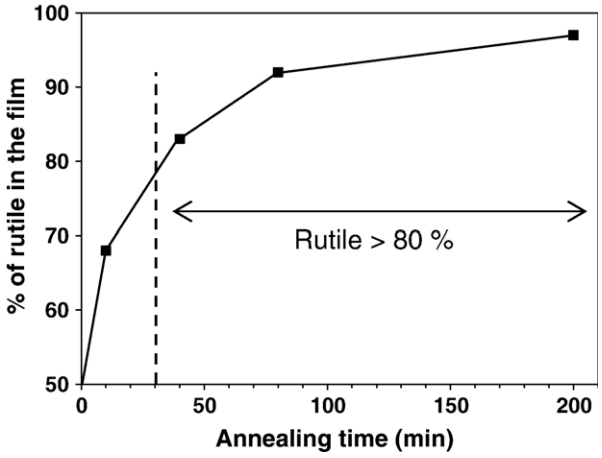

Fig. 8. Rutile amount determined by XRD after oxidation at 823 K of $TiO_{1.5}N_{0.5}$ films grown on Si(100) as a function of the annealing time.

4. Discussion

Oxidation at high temperature (673–823 K) in air of $TiO_{1.5}N_{0.5}$ coatings results in the growth of a TiO_2 top layer with a quasi-linear increase of its thickness until the nitrogen is completely removed. This contrasts with the oxidation kinetics of TiN which was found logarithmic at low temperature ($\leq$100 °C) [20] and quadratic both in the mid-temperature range of 623–723 K [21] and at high temperature (773–923 K) [22]. The oxidation of our $TiO_{1.5}N_{0.5}$ coatings is not diffusion controlled. Their amorphous structure induced by high amounts of O vacancies and defects due to the N incorporation during the CVD growth of the oxinitride coatings probably facilitates O diffusion through the growing oxide. The first oscillations in Fig. 3 correspond to the formation of anatase as supported by XRD results and it can be seen from the duration of these oscillations that the oxidation kinetics is thermally activated. The activation energy (19 kcal mol^{-1}) is significantly lower than the values reported for TiN (27–37 kcal mol^{-1}) [21].

Annealing in air at high temperatures leads to the formation of rutile (Fig. 2). Either rutile nucleation occurs directly from $TiO_{1.5}N_{0.5}$ or from the anatase growing film; this last assumption being the most probable. At 823 K an anatase–rutile mixture is observed by XRD in the early stages of the oxidation, then rutile becomes rapidly the dominant phase. After 30 min the relative amount of rutile is higher than 80% (Fig. 8). Interestingly, the period of oscillations is significantly longer after this time suggesting that the second set of oscillations in Fig. 3 would correspond to the anatase–rutile transformation.

This would be consistent with an increase of the rutile thickness by the displacement of an anatase–rutile interface. However the anatase–rutile transformation depends on various

parameters and for instance on the atmosphere [23]. As a result, further studies are necessary to confirm the second set of oscillations observed at high temperature due to anatase–rutile transformation. If this is true, in situ kinetic informations could be obtained by IR pyrometry.

Optical constants (n, k) have been estimated for the TiO_2 layer from in situ pyrometric analysis, *i.e.* at 723 K and at the wavelength of the pyrometer (1.6 μm), and they are in satisfactory agreement with the reflectance measurement achieved ex situ, *i.e.* at room temperature and in the wavelength range 600–850 nm. However a thorough comparison and comments on the wavelength influence is not possible at this stage because sufficient data were not available and the optical constants of TiO_2 depend both on the wavelength and on the temperature [24].

5. Conclusion

Significant variations of the pyrometric signal due to interferences resulting from multi-reflections at the interfaces of an oxide growing film were observed during annealing of $TiO_{1.5}N_{0.5}$ coatings in air. SIMS, XRD and reflectance analyses gave evidences for the growth of TiO_2 as top layer whose thickness increases linearly with the oxidation time. Modeling of the time dependence of the IR pyrometric signal allowed in situ determination of the oxide thickness and transformation rate. This demonstrates that IR pyrometry is a sensitive and very attractive surface diagnostic tool to investigate the reactivity of various materials under severe environment as oxidation at high temperature.

References

[1] P. Pigeat, N. Pacia, B. Weber, Appl. Surf. Sci. 27 (1986) 214.
[2] S. Barrat, P. Pigeat, I. Dieguez, E. Bauer-Grosse, B. Weber, Thin Solid Films 304 (1997) 98.
[3] V. Mortet, A. Kromka, R. Kravets, J. Rosa, V. Vorlicek, J. Zemek, M. Vanecek, Diamond and Related Materials 13 (2004) 604.
[4] S. Barrat, P. Pigeat, I. Dieguez, E. Bauer-Grosse, B. Weber, Thin Solid Films 263 (1995) 127.
[5] Z. Yin, Z.L. Akkerman, F.W. Smith, R. Gat, Mater. Res. Soc. Symp. Proc 441 (1997) 653.
[6] K.A. Snail, C.M. Marks, Appl. Phys. Lett. 60 (1992) 3135.
[7] K. Biermann, A. Hase, H. Künzel, J. Cryst. Growth 201–202 (1999) 36.
[8] A.J. SpringThorpe, T.P. Humphreys, A. Majeed, W.T. Moore, Appl. Phys. Lett. 55 (1989) 2138.
[9] C. Gasqueres, F. Maury, F. Ossola, Chem. Vap. Depos. 9 (2003) 34.
[10] C. Gasqueres, F.-D. Duminica, F. Maury, Chem. Eng. Process. (2007), doi:10.1016/j.cep.2007.01.005.
[11] F. Senocq, F.-D. Duminica, F. Maury, T. Delsol, C. Vahlas, J. Electrochem. Soc. 153 (2006) G1025.
[12] F. Maury, F.-D. Duminica, Thin Solid Films (2007), doi:10.1016/j.tsf.2007.04.007.
[13] P. Pigeat, D. Rouxel, B. Weber, Phys. Rev. B 57 (1998) 9293.
[14] F. Benedic, P. Bruno, P. Pigeat, Appl. Phys. Lett. 90 (2007) 134104.
[15] F.-D. Duminica, F. Maury, R. Hausbrand, Surf. Coat. Technol. (2007), doi:10.1016/j.surfcoat.2007.04.061.
[16] N. Kumar, K. Pourrezaei, B. Lee, E.C. Douglas, Thin Solid Films 164 (1988) 417.
[17] N. Martin, O. Banakh, A.M.E. Santo, S. Springer, R. Sanjines, J. Takadoum, F. Levy, Appl. Surf. Sci. 185 (2001) 123.
[18] S.H. Mohamed, O. Kappertz, J.M. Ngaruiya, T. Niemeier, R. Drese, R. Detemple, M.M. Wakkad, M. Wuttig, Phys. Status Solidi (A) 201 (2004) 90.
[19] M. Screemany, S. Sen, Mater. Chem. Phys. 83 (2004) 169.
[20] C. Ernsberger, J. Nickerson, T. Smith, A.E. Miller, D. Banks, J. Vac. Sci. Technol., A 4 (1986) 2784.
[21] H.G. Tompkins, J. Appl. Phys. 70 (1991) 3876.
[22] M. Wittmer, J. Noser, H. Melchior, J. Appl. Phys. 52 (1981) 6659.
[23] R.D. Shanon, J. Appl. Phys. 35 (1964) 3414.
[24] G. Gulsen, M. Naci Inci, Opt. Mater. 18 (2002) 373.